Nonlocal Pulse Shaping with Entangled Photon Pairs

M. Bellini,[1,4] F. Marin,[2,4] S. Viciani,[1] A. Zavatta,[3] and F. T. Arecchi[2,4]

[1]*Istituto Nazionale di Ottica Applicata, Largo E. Fermi, 6, I-50125, Florence, Italy*
[2]*Department of Physics, University of Florence, Florence, Italy*
[3]*Department of Systems and Computer Science, University of Florence, Florence, Italy*
[4]*Istituto Nazionale per la Fisica della Materia, Unità di Firenze, Florence, Italy*

Nonlocal shaping effects in the time or spectral profiles of an entangled photon pair emerging from a pulsed parametric down-converter are observed by spectrally or temporally filtering one of the twin beams. In particular, we demonstrate the appearance of fourth-order ("ghost") interference fringes in the spectrum of one beam conditioned by photodetection at the output of an unbalanced Michelson interferometer placed in the path of the other beam. The coherence time of the pump is the limiting factor for the sharpness of the details in the shaped biphoton spectrum.

Nonlocal effects in quantum mechanics have been the object of intense speculation and experimental investigation ever since the first discussions by Einstein, Podolsky, Rosen, and Bohr [1,2]. Entangled particle pairs are the fundamental workbench for nonlocal behaviors, and nonlocal correlations have been observed in the polarization, energy, or spatial properties of the pairs. In all such cases, the measurement of an observable on one particle determines the outcome of a conditional measurement performed on the same observable of the other particle of the pair.

Spontaneous parametric down-conversion (SPDC) of laser light in nonlinear crystals is currently the most practical and efficient source of entangled pairs of particles for quantum measurements. Annihilation of a pump laser photon of frequency ω_P and momentum $\mathbf{k}_P$ inside the crystal gives simultaneous birth to a pair of correlated photons, named signal and idler, with frequencies ω_s and ω_i, as well as momenta $\mathbf{k}_s$ and $\mathbf{k}_i$, which must obey energy and momentum conservation ($\omega_P = \omega_s + \omega_i$, $\mathbf{k}_P = \mathbf{k}_s + \mathbf{k}_i$). Thus, although the individual properties of the photons are largely undetermined, their global behavior is unambiguously fixed by the characteristics of the pump and by the conservation laws. Their energies must sum up to the energy of the pump photon, their wave vectors must satisfy the phase-matching condition inside the crystal, and they must be generated at the same time [3].

Although the first optical evidence of nonlocal effects was obtained by violating Bell's-type inequalities [4] in experiments on photon polarization correlations [5], several others have followed that put into evidence the striking nonlocal correlations due to energy-time or momentum-space entanglement. Experiments of the kind first suggested by Franson in 1989 [6–9] have shown the nonlocal character of the two-photon (or biphoton) quantum state by the observation of fourth-order interference effects among distant interferometers, due to the time-energy correlations in the photon pairs. On the other hand, the correlation between the emission directions of entangled pairs has been clearly demonstrated by experiments on "ghost" interference and diffraction [10–13], where positioning a double slit in the path of one of the beams nonlocally causes the other beam to show Young's type interference patterns.

Here we present experiments which are the time-domain counterpart of those on ghost interference and diffraction. By either spectrally or temporally shaping one of the two beams emerging from a parametric crystal, we show that the other beam of the pair is, respectively, temporally or spectrally shaped, when observations are made in coincidence.

Our experimental apparatus is schematically drawn in Fig. 1. The 4–5 ps long pulses from a mode-locked Ti:sapphire laser, operating around 788 nm at a repetition rate of about 82 MHz, are frequency doubled in a LBO
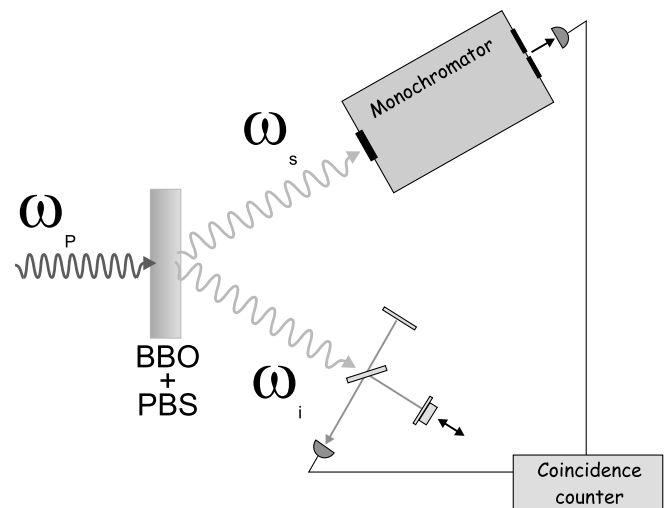
FIG. 1. Simplified scheme of the experiment. See the text for details.

(lithium triborate) crystal to generate the pump pulses for SPDC. About 25–30 mW of the resulting blue light is mildly focused on a 3-mm-long BBO (beta barium borate) crystal cut for type-II collinear degenerate down-conversion. The crystal is slightly tilted from the collinear condition in order to have the two orthogonally polarized beams emerging from the crystal in the form of separated quasi-Gaussian spots as in [14]. After being recollimated and separated by a polarizing beam splitter (PBS), one of the beams (we will name it the "signal" in the following) is sent to a 500-mm monochromator allowing for a spectral resolution of about 0.02 nm, while the other (the "idler") is directed to a stable Michelson interferometer with piezo-controlled arm movements. At the exit of both the spectrometer and the interferometer, single-photon counting modules (SPCM, EG&G AQR-12) are placed, where all the emerging light is collected by means of short focal-length lenses. In order to cut some of the background, 5-nm bandwidth interference filters are placed in front of the detectors.

The signals from the two SPCMs can be either counted directly or in coincidence as a function of some parameters: the center wavelength and width of the spectral filter given by the monochromator, or the relative path-length difference between the two arms of the interferometer.

By observing a single channel, the spectrum or the coherence time of the down-converted photons can be measured. The coherence time of the pulses is obtained by measuring the first-order autocorrelation function with the Michelson interferometer and by extracting the width of the visibility curve of the resulting fringes. A FWHM spectral width of 4.5 nm and a corresponding coherence time of about 200 fs are measured on the signal and idler beams. In such cases, the widths and shapes of the resulting curves are essentially determined by the combined effect of the transmission of the interference filters placed in front of the detectors, and of the phase-matching-limited bandwidth of the parametric fluorescence.

If observations are made in coincidence, fourth-order interferences are investigated, yielding quite different results. Let us consider first the case when the monochromator wavelength is set near the peak of the filter transmission curve, with a fixed slit width, while the temporal delay is scanned in the interferometer. When narrowing the exit slit, fourth-order interference fringes of good visibility start to appear even at large time delays, indicating that the coherence time of the correlated photon is getting longer.

Similar effects have been known for a long time [3,15] and are explained in the frame of quantum mechanics by the collapse of the entangled-state wave function

$$|\psi\rangle = \int_0^\infty \int_0^\infty d\omega_s d\omega_i \delta(\omega_P - \omega_s - \omega_i) A(\omega_s, \omega_i) |\omega_s\rangle |\omega_i\rangle \tag{1}$$

to the state

$$|\omega_s\rangle |\omega_P - \omega_s\rangle, \tag{2}$$

when the frequency of the first photon is measured to be ω_s. In the above expressions $A(\omega_s, \omega_i)$ is the probability amplitude for the generation of a pair of conjugated photons at frequencies ω_s and ω_i, and the energy conservation law is introduced by means of the δ function in Eq. (1).

If the pump were a perfectly monochromatic field as assumed in (1), the bandwidth of the idler photon would be exactly equal to that of the spectral filter placed in the path of the signal. However, a pulsed radiation experiment implies a finite bandwidth of the pump. Thus, at high frequency resolutions, corresponding to long delay times within the Michelson interferometer, the monochromatic pump assumption of (1) and (2) fails. The bandwidth of the pump can be simply taken into account by an integration over the pump spectrum [16–18]. In general, the coherence time of the idler is obtained from the autocorrelation function defined as

$$\hat{\Gamma}_i(\tau) = \int dt E_i^-(t - \tau) E_i^+(t) \tag{3}$$

with

$$E_i^+(t) = \int d\omega_i e^{i\omega_i t} \hat{a}_{\omega_i}. \tag{4}$$

Its average value can be calculated by tracing over the density matrix of the photon state on the idler channel, which is given, e.g., in Refs. [19,20]. It is then easily found that the resulting function is the inverse Fourier transform of the convolution of the pump spectrum with the monochromator filter. As a consequence, however narrow is the filter on the signal photon, the correlated spectral width of the idler is always found to be limited to the bandwidth of the pump. If the pump pulse is Gaussian with a FWHM $\Delta\omega_P$, the visibility of the fourth-order interference fringes reduces to $1/2$ for a delay corresponding to the pump coherence time $\tau = 4\ln2/\Delta\omega_P$. We measured τ to be about 2.9 ps, corresponding to a bandwidth of approximately 0.3 nm at the signal wavelength.

We performed measurements of the autocorrelation function of the idler photon for different values of the spectral resolution of the monochromator. Results are presented in Fig. 2(a), where the visibility of the fourth-order interference fringes as a function of the delay between the two arms of the Michelson interferometer is plotted. The expected shape of the visibility curve for an infinitely narrow spectral resolution of the monochromator is also shown as a solid curve.

Figure 2(b) shows the coherence times extracted from the idler autocorrelation curves, as a function of the width of the exit slit of the monochromator placed on the signal beam path. The temporal coherence of the idler grows with the inverse of the filter bandwidth while this is larger than the bandwidth of the pump pulse. When
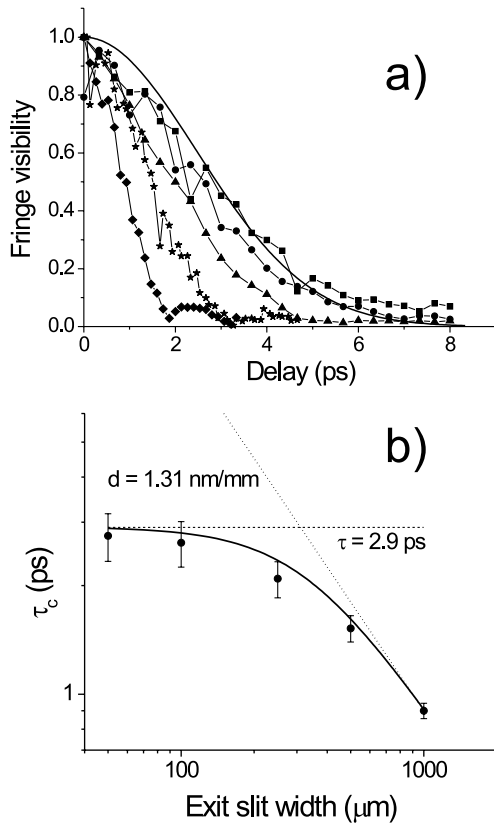
FIG. 2.   (a) Experimental visibility of fourth-order temporal interference fringes on the idler beam for different values of the monochromator output slit width in the signal channel (diamonds 1 mm; stars 500 μm; triangles 250 μm; circles 100 μm; squares 50 μm). The input slit width is set to 50 μm. The solid line is the limit curve, calculated assuming a Gaussian pump spectrum with the measured bandwidth. (b) Coherence times of the idler photon. The solid curve is calculated from the experimentally available pump coherence time (horizontal dashed line) and monochromator dispersion (dotted line).

the spectral resolution of the monochromator is reduced below the pump bandwidth, it approaches a constant value, corresponding to the measured coherence time of the pump. Experimental data are well reproduced by the calculated solid line, obtained considering the convolution of the Gaussian pump spectrum with the monochromator spectral filter. For this filter we have assumed a rectangular shape with a width given by the slits and by the measured value of the monochromator dispersion $d = 1.31$ nm/mm.

A complementary experiment can be performed with the same apparatus. This time we fix the time delay T between the interferometer arms and scan the wavelength of the monochromator, thus measuring the spectrum of the signal photon conditioned on the detection of an idler photon after the Michelson.

Considering pump pulses with a coherence time τ, it is intrinsically impossible to decide which of the two

arms of the interferometer was traveled by the idler photon if $T < \tau$, whether generated at time t_0 within the pump pulse and then traveled the long interferometer arm or generated at $t_0 + T$ (still within the pump coherence time), and then passed through the short arm. The observation of an idler photon at the exit of the interferometer then collapses the state of the signal photon onto a coherent superposition of pulses born at times t_0 and $t_0 + T$, with t_0 undetermined but with a fixed separation T. The spectrum of such phase-locked and time-delayed signal pulses is given by the broad envelope of the transmission curve of the interference filters, modulated in a sinusoidal way with a period proportional to the inverse of the time delay T.

If the delay T is made longer than τ, then either the birth time t_0 or $t_0 + T$ lies outside the coherence time of the pump, and the corresponding quantum path simply vanishes. In such cases it is in principle possible to distinguish between the two alternative paths of the idler photon in the interferometer, and the modulation in the corresponding signal spectrum disappears. As long as narrow input and output monochromator slits are used (such that the signal detector sees only a spectral portion smaller than the fringe period $\Omega = 2\pi/T$ at a time), then it is this intrinsic distinguishability of the two quantum alternative paths that causes the decrease in the fringe visibility rather than the limited instrumental resolution.

Alternatively, one may think that the effect of the Michelson interferometer is that of introducing a sinusoidal spectral filter with a variable period Ω in the idler path. As the idler photons are detected at the exit of the interferometer, the spectrum of the signal is correspondingly collapsed to a periodically modulated one. In the case of a monochromatic pump with an infinite coherence time, only the finite spectral resolution of the monochromator would put a limit to the maximum achievable delay of the interferometer to still observe spectral modulations.

Figure 3 shows a few spectra obtained for different values of the time delay T. Fourth-order spectral interference fringes are evident in the coincidence spectra, while no modulation is observed in the singles' counts for the signal pulse. Note that for particular values of the time delay T, it is possible to dig a deep hole in the center of the two-photon spectral profile, down to nearly vanishing coincidence counts. Visibilities higher than 80% are observed in the spectra. In such cases [see, for example, Fig. 3(b)], the outputs of the interferometer and of the monochromator exhibit a nearly complete anticorrelation and no photon at a particular wavelength is to be expected in coincidence with a photon out of the Michelson.

Our results are the temporal counterpart of those obtained by several authors on the phenomenon of nonlocal (ghost) interference and diffraction in the spatial domain. Indeed, our experiments exploit the time-energy
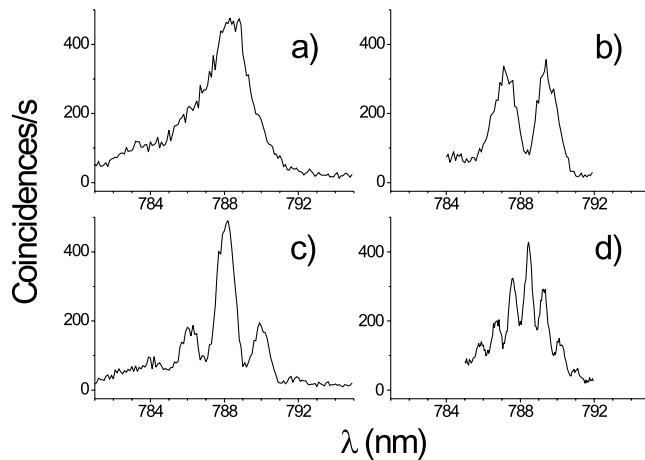
FIG. 3. Fourth-order spectral interference fringes on the signal spectrum conditioned on the detection of an idler photon after the Michelson interferometer. Data are taken with monochromator slit widths of 100 (input) and 250 μm (output). Figures correspond to time delays between the interferometer arms of (a) ~0 fs, (b) 700 fs, (c) 1000 fs, and (d) 2300 fs.

entanglement of the photon pairs instead of the space-momentum correlations used by Strekalov *et al.* [10], but the final results show an impressive resemblance and clearly indicate the same underlying physics.

Placing a single slit of variable width in the path of one photon and observing the two-photon diffraction pattern on the other is analogous to our spectral filtering on one channel and to the observation of the temporal stretching in the two-photon interferogram.

Conversely, the role of the Young's double slit in the spatial version is played in our case by the Michelson interferometer, which represents a sort of temporal double slit. The observation of the far-field pattern of the second photon corresponds to the measurement of the frequency spectrum performed by the monochromator in our experiment. Also, in the spatial version of the experiment, the transverse coherence of the pump beam is the limiting factor for the maximum distance between the slits, just like the (longitudinal) temporal coherence of the pump pulse sets the maximum delay in our interferometer to still observe fourth-order interferences.

In summary, we have performed systematic measurements of the spectral and temporal shaping effects on one photon of an entangled pair in response to observations made on the other member of the pair. In particular, we have demonstrated the appearance of high-visibility fourth-order interference fringes in the spectral profile of the biphoton.

Our basic shaping mechanisms can be in principle extended to much more complicated situations, including the use of adaptive techniques based on spatial light modulators [21]. Similar devices, now widely used in the field of atomic and molecular coherent control, might be exploited, for example, to optimize the spectral/temporal matching between the down-converted pulses and those coming from a local oscillator in a homodyne-type measurement, in order to improve the global efficiency of the system.

By the use of a pulsed pump source in our experiments, we have brought to evidence the effect of a finite (and large, in our case) pump bandwidth on the process; we have shown that the coherence time of the pump pulses limits the maximum extension of the nonlocal temporal modulations which may be imposed on the down-converted beams and, complementarily, that the spectral width of the pump sets the magnitude of the finest details encoded in the nonlocally modulated spectrum.

---

[1] A. Einstein, B. Podolsky, and N. Rosen, Phys. Rev. **47**, 777 (1935).
[2] N. Bohr, Phys. Rev. **48**, 696 (1935).
[3] D. C. Burnham and D. L. Weinberg, Phys. Rev. Lett. **25**, 84 (1970).
[4] J. S. Bell, Physics (Long Island City, N.Y.) **1**, 195 (1964).
[5] A. Aspect, J. Dalibard, and G. Roger, Phys. Rev. Lett. **49**, 1804 (1982).
[6] J. D. Franson, Phys. Rev. Lett. **62**, 2205 (1989).
[7] Z. Y. Ou, X. Y. Zou, L. J. Wang, and L. Mandel, Phys. Rev. Lett. **65**, 321 (1990).
[8] P. G. Kwiat, W. A. Vareka, C. K. Hong, H. Nathel, and R. Y. Chiao, Phys. Rev. A **41**, 2910 (1990).
[9] J. Brendel, E. Mohler, and W. Martienssen, Phys. Rev. Lett. **66**, 1142 (1991).
[10] D. V. Strekalov, A. V. Sergienko, D. N. Klyshko, and Y. H. Shih, Phys. Rev. Lett. **74**, 3600 (1995).
[11] R. Christanell, H. Weinfurter, and A. Zeilinger, The Technical Digest of the European Quantum Electronic Conference EQEC's93, Florence, 1993 (unpublished), p. 872.
[12] P. H. Souto Ribeiro and G. A. Barbosa, Phys. Rev. A **54**, 3489 (1996).
[13] E. J. S. Fonseca, P. H. Souto Ribeiro, S. Pádua, and C. H. Monken, Phys. Rev. A **60**, 1530 (1999).
[14] S. Takeuchi, Opt. Lett. **26**, 843 (2001).
[15] P. G. Kwiat and R. Y. Chiao, Phys. Rev. Lett. **66**, 588 (1991).
[16] J. G. Rarity and P. R. Tapster, Phys. Rev. A **45**, 2052 (1992).
[17] Z. Y. Ou, Quantum Semiclass. Opt. **9**, 599 (1997).
[18] A. V. Burlakov, M. V. Chekhova, O. A. Karabutova, and S. P. Kulik, Phys. Rev. A **63**, 053801 (2001).
[19] T. Aichele, A. I. Lvovsky, and S. Schiller, Eur. Phys. J. D **18**, 237 (2002).
[20] M. H. Rubin, Phys. Rev. A **61**, 022311 (2000).
[21] See, for example, A. M. Weiner, Rev. Sci. Instrum. **71**, 1929 (2000), and references therein.